A Comparative Study of the EBIC Contrast and Gettering Efficiency of the Tilt Boundaries Σ= 25, Σ= 13 and Σ= 9 in Silicon Bicrystals

A. Ihlal, R. Rizk, P. Voivenel, G. Nouet

Classification
Physics Abstracts
61.70N — 68.22 — 72.20J

A Comparative Study of the EBIC Contrast and Gettering Efficiency of the Tilt Boundaries $\Sigma = 25$, $\Sigma = 13$ and $\Sigma = 9$ in Silicon Bicrystals

A. Ihlal(*), R. Rizk(**), P. Voivenel and G. Nouet

LERMAT, URA CNRS 1317, ISMRA, 6 Bd du Maréchal Juin, 14050 Caen Cedex, France

(Received 19 December 1994, revised 9 March 1995, accepted 23 March 1995)

Résumé. — Des mesures EBIC (Electron Beam Induced Current) ont été réalisées sur des bicristaux de silicium contenant les joints de flexion $\Sigma = 25$, $\Sigma = 13$ et $\Sigma = 9$, afin d'étudier l'activité recombinante des précipités de nickel dans ces matériaux. Parallèlement, une étude comparative de l'efficacité de "gettering" de ces joints a été abordée. Les différents aspects du contraste EBIC (uniforme, uniforme et ponctué ou simplement ponctué) ont été corrélés à la microstructure des interfaces, laquelle gouverne la taille et la distribution des précipités de $NiSi_2$. En outre, l'apparition et l'étendue de la zone dénudée de part et d'autre du joint ont été toutes deux associées à l'efficacité de "gettering" de chaque type de joint, laquelle a été trouvée tout à fait compatible avec les valeurs calculées de l'énergie libre du joint.

Abstract. — Electron Beam Induced Current (EBIC) measurements have been performed on $\Sigma = 25$, $\Sigma = 13$ and $\Sigma = 9$ silicon bicrystals, aiming at the study of the recombining activity of nickel precipitates in these materials, together with a comparative study of the gettering efficiencies of the related Grain Boundaries (GBs). The various aspects of the EBIC contrasts such as their strength and nature (uniform, uniform and dotted or dotted only) have been correlated to the microstructure of the interfaces, which govern the size and distribution of the $NiSi_2$ precipitates. On the other hand, the appearance and the extent of a denuded zone on either side of the GB have been both associated with the gettering efficiency of each of GB-type, which was found to account for the corresponding free-energy of the GB as theoretically calculated in the literature.

1. Introduction

The large amount of studies undertaken so far on polycrystalline semiconductors has demonstrated that Grain Boundaries (GBs) control closely the transport mechanisms in these materials [1]. This observation has motivated the numerous investigations devoted to the microstructure analysis and electronic behaviour of GBs. In this connection, the electrical activities of

(*) *Permanent address: Département de Physique, Faculté des Sciences, B.P. 28/S, Agadir, Morocco*
(**) To whom correspondence should be addressed.

typical GBs in silicon such as the coincidence boundaries in specially grown bicrystals are now widely attributed to extrinsic origin i.e. to impurities [2]. The role of these latter is revealed very often through the silicides formed at the GB upon heat treatment and whose origin is the nonintentional [3,4] or deliberate [5,6] contamination with metallic elements. Among the various contaminants, copper and nickel have been the object of particular interest inasmuch as both elements are usually thought to be easy contaminants [4].

While some earlier works have been focused on the role of deliberately incorporated copper in the GB electronic states [6] and structure [7] of the particular twin boundary $\Sigma = 25$, we have reported recently some significant contributions to the study of the competing behaviours of Cu and Ni [8] and that of the peculiar effects of nickel only [9] in the same GB ($\Sigma = 25$). There, we have analysed by Thermally Stimulated Capacitance (TSCAP) and Deep Level Transient Spectroscopy (DLTS) measurements the evolution of the barrier heights and the electronic states of the interface as a function of the impurity content [8] and of the treatment temperature [9]. Additionally, the microstructural configurations of the silicon/nickel silicide interfaces have been carefully examined by High Resolution Electron Microscopy (HREM) technique [10]. In order to complement the above-mentioned analyses (TSCAP and DLTS) that dealt with the majority carriers, we have carried out by Electron Beam Induced Current (EBIC) technique a systematic study of the recombining centers in nickel-contaminated silicon bicrystals whose activity is governed by the minority carriers. Here, we shall be concerned with the comparative study of each of the EBIC contrast and gettering efficiency of $\Sigma = 25$, $\Sigma = 13$ and $\Sigma = 9$ silicon bicrystals in combination with Transmission Electron Microscopy (TEM) observations and Energy-Dispersive X-ray (EDX) analyses.

2. Experimental

The samples used in this study were cut from silicon bicrystals supplied by CEN- Grenoble (France). Table I reports the various geometrical characteristics of the specimens such as the twin planes, tilt axes and tilt angles of the investigated GBs. Also indicated are the dopant type and concentration of the corresponding bulk grains. As native impurities, oxygen and carbon have been detected by infrared spectroscopy [11,12] and found to be around 10^{17} cm^{-3} and in the range $1 - 5 \times 10^{17}$ cm^{-3}, respectively. In order to prevent any inadvertent contamination, the samples were chemically etched in an acid bath ($16HNO_3$: $3CH_3COOH$: 1HF) before being nickel plated by chemical reaction with a $NiSO_4$ solution. They were then submitted to annealing in a thoroughly cleaned double-wall quartz tube furnace under continuous flow of

Table I. — *Geometrical characteristics of the twin boundaries* $\Sigma = 25$, $\Sigma = 13$ *and* $\Sigma = 9$ *GBs in silicon bicrystals. Also reported are the dopant type and concentration in the grains.*

Σ	Twin plane	Tilt angle	Tilt axis	Type	dopant concentration
25	{710}	16.2°	[001]	n	3.1×10^{14} P/cm^3
13	{510}	22.6°	[001]	n	5×10^{14} P/cm^3
				p	6.5×10^{14} P/cm^3
9	{122}	38.9°	[011]	p	6.5×10^{14} P/cm^3

pure argon for 3 h at 1100 °C. Subsequently, the samples were rapidly cooled by withdrawing them from the furnace to the cold end of the quartz tube.

For EBIC measurements, the samples were mirror-like polished and chemically etched prior to the deposition of the appropriate Schottky diodes. Three of these latter have been realized on each sample, one at the GB and one on each of the adjacent grains, by deposition of either gold (for n-type) or chromium (p-type) on the front surface. The ohmic contact was achieved with the eutectic GaAl alloy on the scraped back surface. The EBIC experiments have been performed in a Scanning Electron Microscope (SEM) operating in the range 15-35 KV with an electron beam intensity of 1 nA. Most of our investigations were performed at the higher beam energy (35 kV), leading to an electron penetration as deep as ~ 8 μm which have enabled us to explore the neutral zone of the semiconductor, i.e. well beyond the space charge region that ranges between 1 and 2 μm. Finally, several samples were thinned by ion-milling for TEM observations and EDX analyses.

3. Results

All the as-received and slowly cooled samples exhibited a very weak and uniform contrast of a few percents at the level of their boundaries (1-2% for $\Sigma = 9$, 7% for $\Sigma = 13$, and 4% for $\Sigma = 25$) as reported earlier [11], whereas the bulk grains were almost free from recombining centers. The corresponding conventional TEM observations did not reveal any defect neither at the GBs nor in the bulk. Thus, all the EBIC measurements reported below will concern exclusively the heat-treated samples.

$\Sigma = 25$

The EBIC data of the as-delivered $\Sigma = 25$ type n specimen (not shown here) confirm those reported previously for annealing at 950 °C [11, 12]. They consist in a uniform contrast of about 40% near the GB and the absence of a visible variation of the recombination activity in the bulk. The contrast value associated with a defect can be defined such that $C = (I_0 - I_d)/I_0$, where I_d and I_0 are the current at the defect position and away from the defect, respectively. As for the nickel-contaminated sample, the EBIC images reveal an intense activity both in the bulk (Fig. 1a) and in the GB (Fig. 1b). While the contrast at the interface is fairly uniform, as evidenced clearly by the modulated EBIC image of Figure 1c, and exceeds 50%, the variation of the grey levels of the homogeneously distributed defects in the bulk is indicative of the different location depths of the recombining centers or different defect strenghts [13,14]. The comparison exhibited by the grey levels of Figures 1a, 2a and 2b that have been taken at the accelerating voltages 35, 25 and 15 kV, respectively, seems to suggest a certain depth repartition of the recombining centers. According to Figures 1b and 1c, one can notice the existence on both sides of the GB of a region free of defect or precipitates, commonly called Denuded Zone (DZ) which is exempt from any detectable recombination. The average width of this zone for the present $\Sigma = 25$ sample is estimated to about 150 μm on each side of the GB.

$\Sigma = 13$

Similar measurements on the nonintentionally or deliberately contaminated $\Sigma = 13$ samples n type and p type have given a quite characteristic double contrast (Fig. 3) at the GB, consisting in a background of Uniforme Contrast (UC) to which is superposed a Dotted Contrast (DC). A clear evidence of this aspect is given by the modulated and inverted EBIC image of Figure 3b. Furthermore, from the comparison of the EBIC line profiles for both kind of samples (Fig. 4),

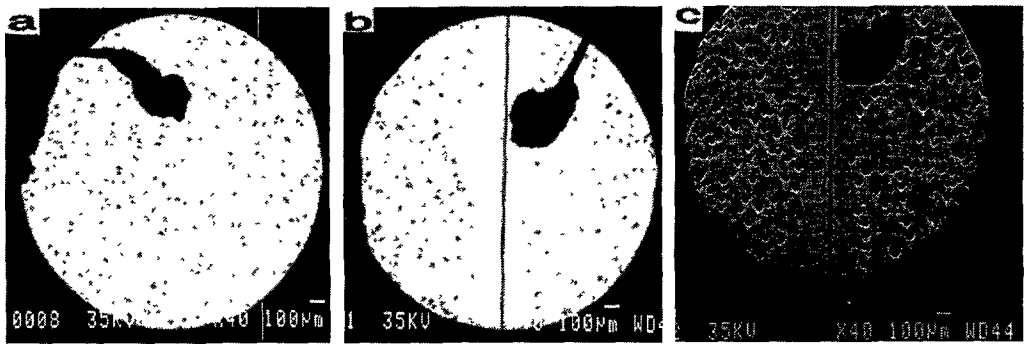

Fig. 1. — EBIC images of the Ni-contaminated $\Sigma = 25$ sample showing the recombining activity of the defects in the bulk a) and at the GB b). c) Represents the modulated EBIC contrast of the zone displayed by b). Electron beam energy: 35 kV.

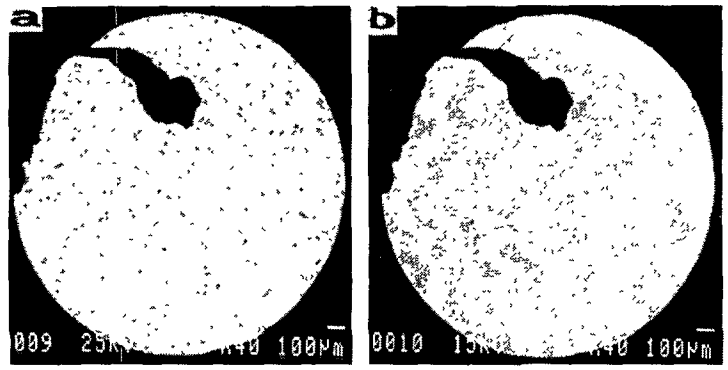

Fig. 2. — The same as in Figure 1a with the beam energies: 25 kV a) and 15 kV b).

one can notice that, regardless of the contamination degree, the contrast revealed at the dot crossing, i.e. the DC, is higher than that exhibited upon scanning the uniform background, i.e. the UC. In addition, there is a substantial increase with contamination of the levels of each of the UC and DC contrasts (Fig. 4).

Nevertheless, the most important aspect lies in the emergence, as for the $\Sigma = 25$, of an intense activity in the bulk for solely the contaminated sample. This is accompanied by the distinction of a DZ (Fig. 3) which recall the similar one observed in $\Sigma = 25$, but extending here to about 120 μm on each side of the GB. The last feature concerns the difference in the defect distribution between the n- and p-types of $\Sigma = 13$ specimens. The density of the recombining centers in p-type material appears notably lower than that in n-type grains, which seems to be compensated by the larger size of the defects (Fig.5).

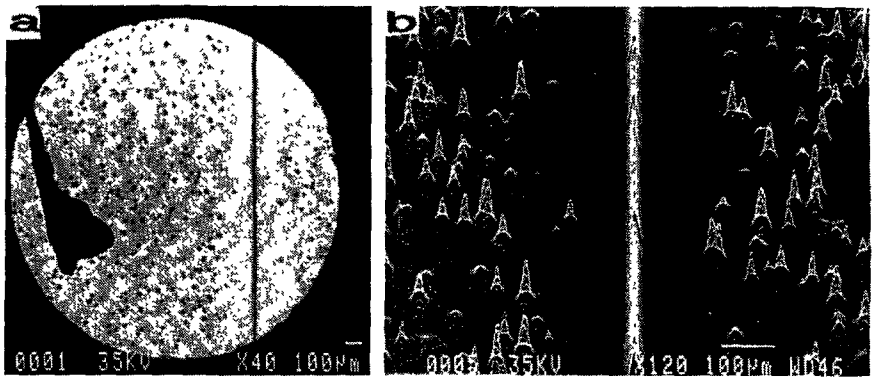

Fig. 3. — a) EBIC image of Ni-contaminated $\Sigma = 13$ n-type sample displaying the GB region. b) reproduces a part of a) in the modulated and inverted mode. Note the different scales between a) and b).

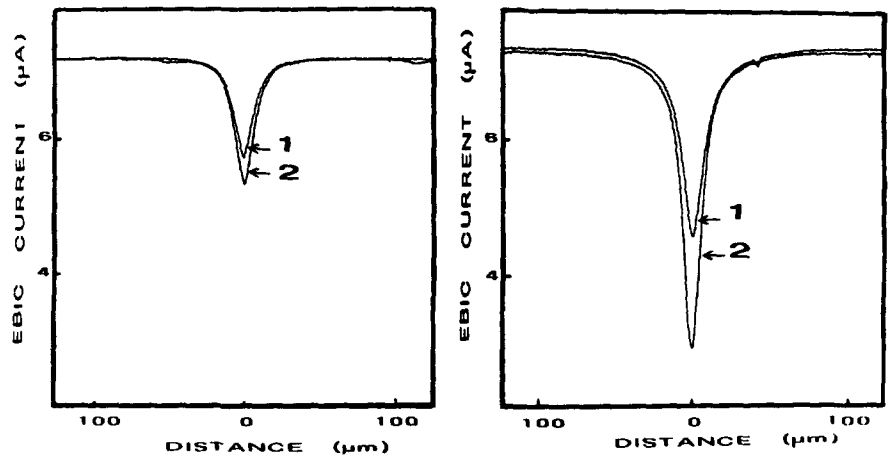

Fig. 4. — EBIC scan profiles across the $\Sigma = 13$ GB of the: a) unintentionally contaminated sample and b) the Ni-contaminated specimen. (1: across a line between dots; 2: across a dot).

$\Sigma = 9$

We report in Figures 6a and 6b the EBIC images of the $\Sigma = 9$ p-type samples relative to the as-received and contaminated with nickel, respectively. It stands out that we are dealing in both cases with a contrast of dotted character only, which is, obviously, much more pronounced for the contaminated specimen. While the contrast value does not exceed a few percent upon scanning between the dots for both kinds of samples, it increases notably at the dot level when nickel is incorporated (Fig. 7). It is worth notice that, following the above-mentioned

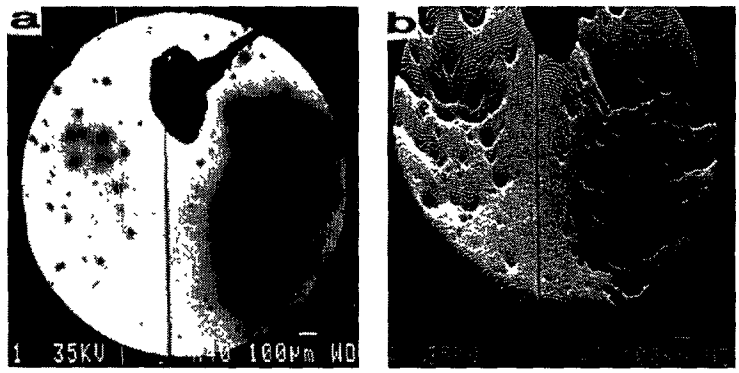

Fig. 5. — a) EBIC image of the GB region of $\Sigma = 13$ p-type sample precontaminated with nickel. b) reproduces the image of a) in the modulated mode.

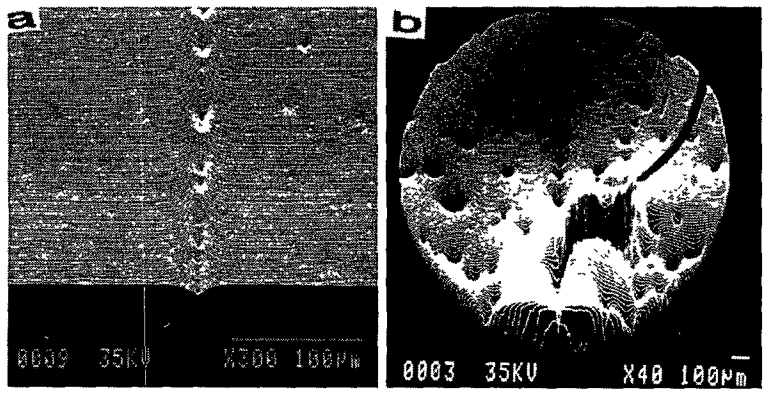

Fig. 6. — Modulated EBIC image of the as-received a) and Ni-contaminated b) $\Sigma = 9$ samples. Note the different scales between both figures.

observations for $\Sigma = 25$ and $\Sigma = 13$, the contamination of $\Sigma = 9$ led to a marked activity of the recombining defects in the bulk whose distribution and average size recall the corresponding ones noticed for the other specimen of the same type, $\Sigma = 13$ type p. For this type, the density of the defect revealed by EBIC images agrees well with that provided by TEM observations. By contrast, one can not recognize from Figure 6b the existence of a DZ comparable to those found in the similarly contaminated $\Sigma = 25$ and $\Sigma = 13$ samples. The repartition of the recombining centers appears rather random without any preferential gettering role for the $\Sigma = 9$ GB.

Since the diffusion length of the minority carriers in the Ni-contaminated and similarly doped samples, as reported by Kittler *et al.* [14], exceeds the average size of the generation volume, we feel well founded to proceed to a comparison of the contrast values. Table II summarizes these values as measured at the GB level upon scanning either across the uniform background or across a dot, and that in both unwantedly contaminated and Ni-contaminated samples.

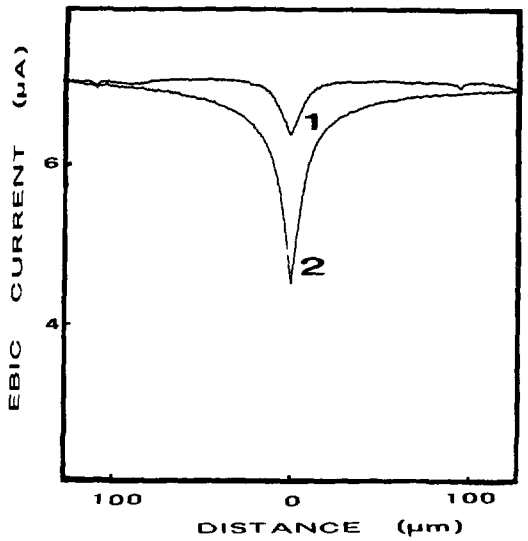

Fig. 7. — EBIC scan profiles across a dot at the level of the GB in a $\Sigma = 9$ unwantedly contaminated (1) and that intentionally contaminated with nickel (2).

Table II. — *Electrical data after heat-treatment at 1100 °C of the nonintentionally and Ni-contaminated samples. UC: Uniform Contrast, DC: Dotted Contrast. The values between parenthesis represent the EBIC contrast (in %).*

Sample	contrast (%)	
	nonintentionally contaminated	Ni-contaminated
Σ=25n	UC (40)	UC (>50)
Σ=13 n and p	UC (20) + DC (28)	UC (36) +DC (60)
Σ=9p	DC (10)	DC (37)

4. Discussion

The variety of situations examined in the above-described results leads us to point out the following salient features: (i) the effect of the intentional contamination with nickel on the emergence of the electrical activity noticed in the bulk and on the increase of that at the GBs, (ii) the various aspects of the contrasts exhibited by the different GBs, namely: uniform

($\Sigma = 25$), uniform and dotted ($\Sigma = 13$) or merely dotted ($\Sigma = 9$), and finally, (iii) the appearance and the extent of the so-called DZ in most of the samples ($\Sigma = 25$ and $\Sigma = 13$, for instance) which could be associated, as discussed later, with the gettering efficiency of the GB.

Unlike the case of the heated as-grown samples where any defect or precipitate has been observed by TEM, and that neither in the bulk nor in the GB, the Ni- contaminated bicrystals have been found to contain small and large plates of nickel silicides. The EDX analyses quoted in our previous works [9,10] and confirmed here demonstrated that we are dealing with $NiSi_2$ growing on Si {111} planes. Thus, whether the substantial increase in EBIC contrast noticed at the GB or, above all, the high electrical activity detected in the bulk, whose contrast approached 50%, they seem both to be due to $NiSi_2$ particles. These latter belong, as reported earlier by many authors [15–17] and recognized also by us [9,10] to the two well-known types of precipitates: the perfectly aligned type A and the twin type B. Their recombination properties in the bulk, as evoked above, are in good agreement with the findings of Kittler *et al.* [14].

As for the important issue regarding the achievement of large precipitates attaining a few μm in p-type whereas the average size of those formed in n-type does not exceed 500 nm [9], it could be correlated to an eventual higher density of nucleation or gettering sites in n-type which limit the growth of its precipitates. Previous works of Ourmazd and Schröter [18] have shown that in phosphorus containing samples (n-type), P gettering (SiP formation) and intrinsic gettering (SiO_x formation) have a similar gettering mechanism. These authors demonstrated that, for Ni-contaminated sample, the gettering Ni nucleated $NiSi_2$ particles which are closely associated with SiP and SiO_2 particles. These latter act as nucleation sites for $NiSi_2$, even when they did not contain any dislocations around them [18]. Therefore, one can speculate that the high number of nucleation or gettering sites in the bulk of n-type could be associated with the additional presence of SiP particles. This would lead, as suggested above, to some limitation of the growth of $NiSi_2$ particles in n-type whereas the silicides could extend in p-type.

Concerning the basic electrical activity detected at the GB in the nickel-free sample, one could be tempted by the assignment of this activity to native impurity and/or Oxide Precipitates (O_{Ps}) which could be formed in our CZ material. Beside the eventual influence of oxygen on the mechanism [19] and morphology [18] of metal precipitates, the role of O_{Ps} in the lifetime degradation has been systematically studied by Hwang and Schroder [20]. In spite of their oxygen-enriched material, these authors noticed the small size of their O_{Ps} (< 100 Å in diameter). Hence, it is quite conceivable that such particles would be even smaller and less numerous in our material because of its lesser oxygen content. In such a case, the size of the eventually existing defects and the concentration of possible precipitating contaminants would be below the detection limit of our investigation techniques (TEM, EDX).

Turning now to the various EBIC contrasts, as measured at the level of the different GBs, it is worth noting that, although their strength is greatly enhanced by the presence of nickel precipitates at the boundary, their nature, uniform ($\Sigma = 25$), uniform and dotted ($\Sigma = 13$), or dotted only ($\Sigma = 9$), seems inherent to the kind of GB. Thus, in order to give some insight into this correlation, one could suggest an explanation based on the different microstructure of the studied GBs. For $\Sigma = 25$, High-Resolution Electron Microscopy (HREM) observations of this GB in Ge [21,22] reveal the presence, along the interface, of a regular repartition of perturbated areas constituted by an array of dislocations, that are stabilized by zones of high coincidence. The fairly dense distribution of such "dislocation" structure [22] along the GB, as viewed at the EBIC scale, as well as its efficiency in impurity segregation, could explain the uniformity and the strength of the EBIC contrast in $\Sigma = 25$, respectively.

According to HREM observations on Ge [22,23], the $\Sigma = 13$ boundary *is* characterized by numerous structures emerging, for energy cost reasons, during the growth process as this tends

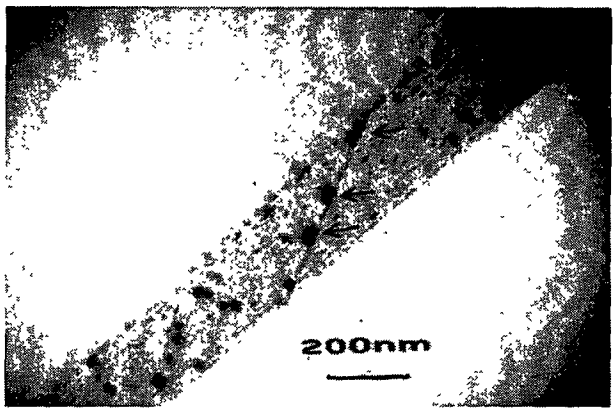

Fig. 8. — TEM micrograph of Ni-contaminated $\Sigma = 13$ sample showing the short facet (indicated by arrows) as decorated by relatively large $NiSi_2$ precipitates. Note the presence of small particles along the GB plane.

to impose a symmetrical {510} interface. Beside long distances ($\sim$ 60 nm) of this symmetrical interface, another asymmetrical {510} interface of high energy, called M structure [22, 23], was observed in small steps. Because of its elevated energy, this short-faceted structure is expected to be a very efficient center for segregation and precipitation. Indeed, Figure 8 gives an illustration of the relatively large nickel precipitates found at the so-called small steps of our $\Sigma = 13$ GB (Fig. 8) and whose formation would be favoured very likely by the presence of the above- mentioned M structure. Consequently, it is reasonable to assign the dotted enhancement in the recorded contrast to these large precipitates, whereas the uniform background might be due to the smaller ones distributed along the boundary (Fig. 8).

A perfectly periodic structure has been found for $\Sigma = 9$ GB which has a glide mirror symmetry as proposed by Hornstra [24] and confirmed later by HREM for Ge [21] and Si [25] bicrystals. Additionally, as no step or defect has been observed in the boundary of the untreated silicon sample [25], it is plausible to consider this structure as the less favourable for segregation and precipitation and would consequently explain the little difference in the distribution of the recombining centers between the bulk and the boundary.

As for the occurrence of a DZ in the neighbourhood of most of the boundaries, as clearly observed for $\Sigma = 25$ and $\Sigma = 13$, it can be originated from the higher free energy in the GBs than in the bulk. This energy excess could be compensated by the segregation and precipitation of impurities, expected to diffuse from the surroundings towards the GB which acts as gettering center. This behaviour leads generally to the "clearing" of the regions adjacent to the GB from the impurities and makes then appear the so-called DZ. The extent of this latter on both sides of the GB could be correlated to the gettering efficiency of the interface, which reflects, in turn, the energy size of the GB. In order to check the consistency between the widths of these DZs and the values relative to the energies of the corresponding GBs, one has to be cautious about the great disparity of the energy values available in the literature. This discrepancy is originated mainly from the use of different computational techniques and/or various interatomic potentials. Only the energy values provided by the same calculation method that calls for the same potential, are comparable. Table III reports the free energy values relating to the most

Table III. — *Energy values of the indicated atomic models of the investigated GBs, as obtained with the use of each of the Keating and Tersoff potentials. a: reference 30; b: reference 22; c: reference 26.*

Σ	Atomic Model	Energy (J/m^2) Keating	Tersoff
5	Z	0.924[a]	0 264[a,b]
9	K	0 60[c]	
13	IH		0 326[b]
	M		0 384[b]
25	SE		0 356[b]
	E		0 366[b]

commonly observed structures of the examined GBs in addition to those of $\Sigma = 5$. These values have been obtained by the use of the indicated potentials but with the same relaxation method at 0 K. It stands out that, with Tersoff potential, the values relating to the so-called SE and E configurations of $\Sigma = 25$ are notably higher than that corresponding to the minimum, so-labeled IH, configuration of $\Sigma = 13$. This would explain the higher gettering efficiency of the former by comparison with that of the latter as seemingly expressed by the wider DZ of $\Sigma = 25$ (150 μm compared to 120 μm for $\Sigma = 13$). On the other hand, the highest energy value corresponding to M configuration appears quite consonant with the attribution of the most elevated contrast (60%, see Tab. II), revealed by the dotted areas at the GB of $\Sigma = 13$, to the asymmetrical {510} interface in short facets where large precipitates have been noticed (Fig. 8).

The final statement concerns the case of $\Sigma = 9$ where no calculation has been performed with the same Tersoff potential whereas the data available in the literature have been obtained by means of Keating potential [26], Density Functional Formalism (DFF) [27,28], tight-binding approximation [27,29] or bond charge model [26]. Nevertheless, as both Keating and Tersoff potentials have been applied for $\Sigma = 5$ [30], one can tentatively adopt a corrective factor enabling the transition between the corresponding calculated values (Tab. III). When applied to the case of $\Sigma = 9$, the just-mentioned correction leads to a fairly low value for its energy (< 0.2 J/m^2) for Tersoff potential, close to that obtained by DFF (0.24 J/m^2) method [27] or that originated from the modified Keating potential [31] and estimated to 0.22 J/m^2 [26]. By comparison with those reported for $\Sigma = 25$ and $\Sigma = 13$ (Tab. III), these low values could then justify the absence of a net DZ in this sample.

5. Conclusion

Summarizing, this work provides a comparative study of the gettering effects of some twin boundaries in silicon bicrystals precontaminated with nickel. The $NiSi_2$ particles have been found to account for the important electrical activity in the bulk and for the notable increase in the EBIC contrast at the grain boundaries. The contrast differences noticed at the level of $\Sigma = 25$ (uniform), $\Sigma = 13$ (uniform and dotted) and $\Sigma = 9$ (dotted only) GBs have been found to originate from the various microstructures of these interfaces, which appeared to govern the precipitation process. Additionally, the gettering efficiency of each boundary was associated with the extent of the denuded zone appearing on either sides of the GB. This zone reached ~ 150 μm for $\Sigma = 25$ and ~ 120 μm for $\Sigma = 13$, whereas it was indiscernible for $\Sigma = 9$. This scaling in the gettering efficiencies have been correlated to a similar ranking in the calculated energy values of the related boundary, as reported in the literature.

Acknowledgments

We are indebted to X. Portier for his assistance in the TEM observations and to O. Hardouin Duparc for enlightening discussions. This work is partially supported by the EC Contract No. SC1*-CT91-0703(TSTS).

References

[1] Polycrystalline Semiconductors III -Physics and Technology, Solid State Phenomena, **37-38**, Strunk H.P., Werner J.F., Fortin B., and Bonnaud O., Eds. (Trans. Tech. Zürich, 1994).

[2] Broniatowski A., "Metal precipitation and the electronic properties of twinned boundaries in silicon", in Intergranular and Interface Boundaries in Materials, Materials Science Forum, **126-128**, Komninou Ph. and Rocher A., Eds. (Trans. Tech. Switzerland, 1993) p. 721.

[3] Hamet J.F., Abdelaoui R., and Nouet G., *J. Appl. Phys.* **68** (1990) 638.

[4] Maurice J.L. and Colliex C., *Appl. Phys. Lett.* **55** (1989) 407.

[5] Broniatowski A., *Phys. Rev. Lett.* **62** (1989) 3074.

[6] Broniatowski A. and Haut C., *Philos. Mag. Lett.* **62** (1990) 407.

[7] Elkajbaji M., Dessus J. and Thibault J., *Philos. Mag. A* **66** (1992) 873.

[8] Rizk R., Portier X., Allais G., and Nouet G., *J. Appl. Phys.* **76** (1994) 952.

[9] Rizk R., Ihlal A., and Portier X., *J. Appl. Phys.* **77** (1995) 1875.

[10] Portier X., Rizk R., Nouet G., and Allais G., *Phil. Mag. A* **71** (1995) 1109.

[11] Ihlal A. and Nouet G., *Phys. Stat. Sol. (a)* **141** (1994) 81.

[12] Ihlal A. and Nouet G., "EBIC contrast and precipitation in annealed silicon bicrystals", in Polycrystalline Semiconductors , Möller H.J., Strunk H.P., and Werner J.H., Eds., Springer Proc. in Physics **35** (Springer, Berlin 1989), p. 77.

[13] Donolato C., *Optik* **52** (1978/1979) 19.

[14] Kittler M., Larz J., Seifert W., Seibt M., and Schröter W., *Appl. Phys. Lett.* **58** (1991) 911.

[15] Seibt M. and Schröter W., *Philos. Mag. A* **59** (1989) 337.

[16] Cherns D., Hetherington J.C.D., and Humphreys J., *Philos. Mag. A* **49** (1984) 165.

[17] Cherns D., Anstis G.R, Hutchison J.L., and Spence J.C.H., *Philos. Mag. A* **46** (1982) 849.

[18] Ourmazd A. and Schröter W., *Appl. Phys. Lett.* **45** (1984) 781; *Mat. Res. Soc. Symp. Proc.* **36** (1984) 25.

[19] Gilles D., Weber E.R., and Hahn S., *Phys. Rev. Lett.* **64** (1990) 196.

[20] Hwang J.M. and Schroder D.K., *J. Appl. Phys.* **59** (1986) 2476.

[21] d'Anterroches C. and Bourret A., *Phil. Mag. A* **49** (1984) 738.

[22] Bourret A. and Rouvière J.L., "Grain boundary structure determination by HREM", in Polycrystalline Semiconductors (see Ref. 12) p. 8.

[23] Rouvière J.L. and Bourret A., "Multiple structure of a [001] $\Sigma = 13$ tilt grain boundary in Ge", in Polycrystalline Semiconductors (see Ref. 12) p. 19.

[24] Hornstra J., *Physica* **25** (1959) 409.

[25] Elkajbaji M. and Thibault-Desseaux J., *Phil. Mag. A* **58** (1988) 325.

[26] Teichler H., "Computer modelling of grain boundaries by use of interatomic potentials", in Polycrystalline Semiconductors (see Ref. 12) p. 25.

[27] DiVincenzo D.P., Alerhand O.L., Schlüter M. and Wilkins J.W., *Phys. Rev. Lett.* **56** (1986) 1925.

[28] Teichler H. and Sanguinetti S., *Phys. Stat. Sol. (a)* **138** (1993) 361.

[29] Thomson R.E. and Chadi D.J., *Phys. Rev. B* **29** (1984) 889.

[30] Rouvière J.L., Thesis (Grenoble, 1989).

[31] Baraff G.A., Kane E.O. and Schlüter M., *Phys. Rev. B* **21** (1980) 5662.